Date of publication xxxx 00, 0000, date of current version xxxx 00, 0000.

Digital Object Identifier 10.1109/ACCESS.2020.DOI

An Ultra-compact X-Band Dual-Polarized Slotted Waveguide Array Unit Cell for Large E-Scanning Radar Systems

NAFATI ABOSERWAL[1,2], (Member, IEEE), JORGE L. SALAZAR-CERRENO[1,2], (Senior Member, IEEE), and ZEESHAN QAMAR[1,2], (Member, IEEE)

[1]School of Electrical and Computer Engineering, The University of Oklahoma, Norman, OK 73019 USA.
[2]Advanced Radar Research Center (ARRC), The University of Oklahoma, Norman, OK 73019 USA.

Corresponding author: Jorge L. Salazar-Cerreno (e-mail: salazar@ou.edu).

ABSTRACT A design of an X-band dual-polarization slotted waveguide antenna (SWGA) array for high polarization performance over 200 MHz bandwidth and wide scan in the azimuth plane, ideal for high-power dual-polarized radar system, is presented. The proposed design uses a compact array unit cell where the overall dimensions are reduced to 50% in comparison with that of the dual-polarization slotted waveguide array antenna using the conventional rectangular waveguides. The new design overcomes the fundamental limitation of zero electronically scanning, due to the large element spacing ($1.2\lambda_\circ$), when conventional waveguides are used. Reducing the element spacing to $0.6\lambda_\circ$ (in the azimuth plane), based on a partial H-plane waveguide, enables a 1D e-scanning range up to $84^\circ(\pm 42^\circ)$ in the azimuth plane perpendicular to the waveguide axis. An active sub-array panel of 8×8 elements, excited with 8 high-power transmit and receive modules, is proposed. This active sub-array can be scaled to obtain a large array without any constraints in size and power. The proposed design uses longitudinal shunt slots on the partial H-plane waveguide for V-polarization antenna and non-inclined edge wall slots on the conventional waveguide for H-polarization antenna. The proposed design offers stable impedance, gain, cross-polarization isolation and excellent co-polar pattern mismatch over the whole frequency band of interest. Having a cross-polarization isolation better than -60 dB and co-polar pattern mismatch around $\pm$ 0.12 dB across the scanning range, make this array unit cell (8x8 elements) a perfect candidate for high power e-scanned dual-polarized phased array radar for weather observations.

INDEX TERMS array, compact antenna, dual-polarization, partial H-plane structure, slotted waveguide antenna, wide scan.

I. INTRODUCTION

MODERN radar and communication systems demand to design an antenna with polarization-agile ability since the polarization diversity can significantly improve the system performance. Dual-polarized phased array antennas with a low sidelobe, high efficiency and low cross-polarization are in demand to improve the observational range and observation accuracy of radar systems [1], [2], and communication systems [3], [4]. In general, the dual-polarized array antennas are mainly formed by the microstrip patch antennas [5]. However, loss performance and some complications with feeding techniques and with materials suitable for environments make slotted waveguide array antennas an attractive alternative solution, in particular at higher frequencies [6], [7]. Slotted waveguide array antennas (SWGAs) have been used for decades, mostly for radar systems in civil and military applications, their use dating at least from the 1950s, therefore their advantages and drawbacks from both the mechanical and the electromagnetic standpoint are well known. Slotted waveguide array antennas guarantee several advantages such as high-gain, low-losses, low-profile, thermal stability, a precise control of aperture excitation, simple feeding, high-power handling, robustness and reliability [8].

The two main types of slotted waveguide array antennas are resonant and traveling wave antennas. In the resonant type, one end or both ends of the waveguide is terminated by short circuit. This results in a standing wave inside the waveguide. In order to have maximum current perturbation

and excite the slot in the waveguide wall, the slot is cut where the maximum electric field is located. In the traveling type, the waveguide is terminated by a matched load to absorb the wave and prevent it from reflection and forming a standing wave. The standing wave (resonant) type of SWGAs is considered in this work [8].

In general, the main antenna configuration of SWGAs with dual-polarization is achieved by interleaving two types of linear SWGAs having orthogonal polarizations, namely, vertical and horizontal. The most basic dual-polarized SWGA architecture can be found in [8]. In this architecture, the same waveguide is used for both vertical and horizontal linear polarizations. It comprises broad wall shunt slots for vertical polarization and inclined edge wall slots for horizontal polarization. Although the architecture is simple and easy to design and manufacture, it has the major drawback of a limited electronic scan capability due to the inter-waveguide spacing and high cross-polarization level, high shoulder and sidelobes, especially for the horizontally polarized array due to the inclined slots. To minimize the presence of the undesired cross-polarization of the inclined edge wall slot waveguide, several designs are developed to replace the inclined edge wall slots with non-inclined edge wall slots [9]. In [10], the excitation of the untilted slots is provided by placing wires inside the waveguide. The untilted slot is excited by a pair of transversely placed tilted wires. These wires are connected between the broad walls and the side walls. The level of the untilted slot excitation is controlled by the separation of these two wires and their tilts. In [11], shaped irises are placed inside the waveguide to excite the untilted slots.

In [12], two parallel waveguides radiating two orthogonal linear polarizations are proposed. The horizontal polarization is realized with an untilted edge wall slot array with slots excited by pairs of irises, while the vertical polarization is realized with a ridged waveguide longitudinal slot array. In this design, the antenna at 9.6 GHz has a scan range of $\pm 23^\circ$ transverse the array axis in the elevation cut with a cross-polarization level more than 25 dB below the main beam peak. In [13], a dual-frequency dual-polarization slotted waveguide array antenna at Ka-band is proposed by interlacing a vertical-polarization longitudinal-slot ridged waveguide array working at 30 GHz and a horizontal-polarization narrow-wall inclined-slot waveguide array working at 35 GHz.

In [14], a broadband dual-polarization slotted waveguide planar array antenna for X-band SAR application is presented. The vertical polarization (VP) is realized with a longitudinal-slot ridged-waveguide linear array antenna, while the horizontal polarization (HP) is realized with an untilted narrow-wall slot linear array excited by shaped irises inside the waveguide. This structure allows $\pm 20^\circ$ beam scanning in across the elevation direction without grating lobes because the width of two linear arrays together is up to $0.7\lambda_\circ$. Another dual-band and dual-polarization slotted waveguide array antenna, designed and tested in the L-band and C-band, is presented in [15]. In this work, the L-band linear slotted waveguide array antenna is employed for single linear polarization which is vertical polarization (VP). However, a dual-polarization slotted waveguide array antenna is designed to work in the C-band. Because the C-band dual-polarization array antenna spacing is about $0.7\lambda_\circ$, this array antenna has a limited-scan up to 40° ($\pm 20^\circ$).

To improve the electronic scan capabilities to $\pm 90^\circ$ in the azimuth direction without grating lobes, the separation of the waveguides in array antenna has to be equal to $0.5\lambda_\circ$. For the use of dual-polarization array antenna, one or both waveguides used for both V- and H-polarizations has to be much narrower than the conventional and ridged ones. To meet the restricted transverse space, this waveguide should be compacted.

In this paper, a dual-polarization slotted waveguide array antenna, ideal for weather radar systems, is presented. The proposed design enables for first time, an unprecedented 1D e-scanning performance to cover 84° ($\pm 42^\circ$) in the azimuth plane. This design provides a co-polar pattern mismatch about ± 0.12 dB between the H- and V-polarization patterns, and cross-polarization isolation better than -60 dB across the scanning range. Therefore, this array unit cell (8x8 elements) can be a perfect candidate for a high power dual-polarized phased array radar for atmospheric applications. The paper is organized as follows: Scanning performance limitations of current dual-polarized SWGAs and the proposed solution are presented in Section II . Then, in Section III, described the design procedure in detail for the vertical polarization and horizontal polarization antennas, separately. After that, the HP and VP linear SWGAs are used to compose the dual-polarization planar SWGA. Finally, a conclusion of this work is shown in Section IV.

II. SCANNING PERFORMANCE LIMITATIONS OF DUAL-POLARIZED SWGAs

A. CURRENT LIMITATIONS OF CONVENTIONAL SWGAs

For planar slotted waveguide array antennas, the antenna beam is electronically scanned in a direction perpendicular to the waveguide axis by phase steering. In this case, each slotted waveguide acts as one element in a one-dimensional scanning array. Inability to fully steer the antenna beam in all directions is one of the sever limitations of this antenna type. However, there are some situations where one-dimensional electronic scan is sufficient for single-polarization planar slotted waveguide array antennas [8].

For single-polarized SWGA antennas, it is also possible to implement electronic beam steering using a conventional waveguide for each polarization (H-polarization or V-polarization), separately in the plane perpendicular to the waveguide axis, for example in [16], the linear array with inclined slots cut in the narrow wall of waveguide for horizontal polarization is traditionally used to compose electronically scanned array along the axis transverse to the waveguide . However, the frequency scanning technique is usually used to scan the beam along the waveguide axis [17], [18]. Frequency or traveling-wave arrays usually offer limited scanning range

(< 20°). Typically those arrays require 200 MHz to 400 MHz, symmetry of beam patterns and low-sidelobe levels are difficult to obtain. For single-polarization planar arrays of radiating longitudinal slots cut in the broad walls of rectangular waveguides may be electronically scanned in the E-plane by including phase shifters between adjacent waveguides. In this case of longitudinal offset slots in the broad walls, the scanning range is limited because of the broad wall dimension being greater than half wavelength in free space. Conventional rectangular waveguides typically have an 'a' broad wall dimension of $0.7\lambda_\circ$ at the operating frequency. Therefore, it is possible to scan the antenna main beam to a maximum angle of 25° off broadside before grating lobes start appearing in the visible space [8]. However, single-polarization planar arrays of radiating transverse slots cut in the narrow walls of rectangular waveguides may be electronically scanned in the H-plane by including phase shifters between adjacent waveguides. These adjacent waveguides with edge wall slots may be placed with a spacing of half wavelength in free space. Therefore, it is possible to scan such arrays electronically over a wide angular range. Conventional rectangular waveguides typically have an 'b' narrow wall dimension of $0.5\lambda_\circ$ at the operating frequency. Therefore, it is possible to scan the antenna main beam to a maximum angle of 90° off broadside before grating lobes start appearing in the visible space [8].

Recently, much attention has paid to wide scan dual-polarization slotted waveguide array antennas due to high power capability and mechanical stability. A dual-polarization feature is achieved by combing side by side two types of linear SWGAs having orthogonal polarizations, namely, vertical and horizontal. The performance of current dual-polarized slotted waveguide array antennas using conventional rectangular waveguides has a major limitation, which is the scan in the plane perpendicular to the waveguide axis is restricted. This is because the center-to-center spacing of the dual-polarized structure is more than one wavelength which will produce grating lobes in case the beam is scanned. Simply, it is impossible to electronically scan in the plane perpendicular to the waveguide axis for no grating lobes being visible using the conventional waveguides.

The maximum element spacing (d_{max}) for the dual-polarized slotted waveguide array antenna scanned to a given scan angle (θ_s) is given by

$$d_{max} = \frac{\lambda_\circ}{\sin\theta_{GL} + \sin\theta_s} \tag{1}$$

where θ_{GL} is the angle of the first grating lobe and $\lambda_\circ$ is the free space wavelength at the operation frequency.

For grating lobe radiation at grazing angle ($\theta_{GL} = 90°$), the equation is expressed as [19]:

$$d_{max} = \frac{\lambda_\circ}{1 + \sin\theta_s} \tag{2}$$

B. PROPOSED SOLUTION USING A COMPACT SWGA ARRAY UNIT CELL

To accomplish a scanning range from -45° to +45° across the used waveguide and avoid grating lobes, compact waveguides for both V- and H-polarizations need to be developed to reduce the unit cell dimension below $0.6\lambda_\circ$. Using the new technique, the unit cell dimension is significantly reduced in comparison with that of the dual-polarization slotted waveguide array antenna using the conventional rectangular waveguides.

TABLE 1: Scanning performance of conventional and proposed dual-polarization linear slotted waveguide antennas using a spacing of $1.2\lambda_\circ$, $0.7\lambda_\circ$ and $0.6\lambda_\circ$ at 9.4 GHz.

	Conventional		Proposed			
	WR-90	WR-90	WR-90	WR-51	Customized	
	H-pol	V-pol	H-pol	V-pol	H-pol	V-pol
Element spacing	$1.2\lambda_\circ$	$1.2\lambda_\circ$	$0.7\lambda_\circ$	$0.7\lambda_\circ$	$0.6\lambda_\circ$	$0.6\lambda_\circ$
maximum scanning	0°		50° (−25° to +25°)		84° (−42° to +42°)	

Fig. 1 shows the grating lobe diagram analysis to illustrate the impact of dual polarization unit cell spacing in the visible region at 9.4 GHz. Fig. 1a,c presents the case for the conventional waveguide structure in azimuth is separated by $1.2\lambda_\circ$. In this case, the grating lobes in azimuth plane fully overlap the visible region at any scanning angle. Therefore, it is impossible to scan the antenna beam without grating lobes appearing in the visible region. Fig. 1c shows that using this spacing for a linear array with 32 elements will produce grating lobes in the visible region eventhough the beam is not scanned. In this case, conventional WR-90 waveguide structures are used for H- and V-polarizations. This work used a compact waveguide structure where the unit cell spacing in azimuth plane can be between $0.6\lambda_\circ$ and $0.7\lambda_\circ$. Fig. 1d,e,f illustrates the grating lobe analysis for both cases. For $0.7\lambda_\circ$, the WR-90 waveguide is used for H-polarization and WR-51 waveguide is used for V-polarization. Because of $0.7\lambda_\circ$ spacing, a scanning range up to $50°$ ($\pm 25°$) in the azimuth cut can be obtained. A $0.6\lambda_\circ$ spacing can be obtained with a customized waveguide structure. This element spacing increases the scanning range up to $84°$ ($\pm 42°$). Fig. 1d,e illustrates both cases, and Fig. 1f shows the ideal scanned patterns of a linear array with 32 elements. Grating lobes appear only when the array is scanned after $\pm 42°$. The scanning performance of a dual-polarization slotted waveguide antenna using a spacing of $1.2\lambda_\circ$, $0.7\lambda_\circ$ and $0.6\lambda_\circ$ is summarized in Table 1.

III. PROPOSED DUAL POLARIZATION ARRAY ANTENNA

In this paper, dual-polarization slotted waveguide array antenna comprises a (VP) linear array and a (HP) linear array. A small array, as an array unit cell, is designed to verify the proposed concept. Both VP and HP linear arrays used to build dual-polarization compact planar array antennas will be explained respectively.

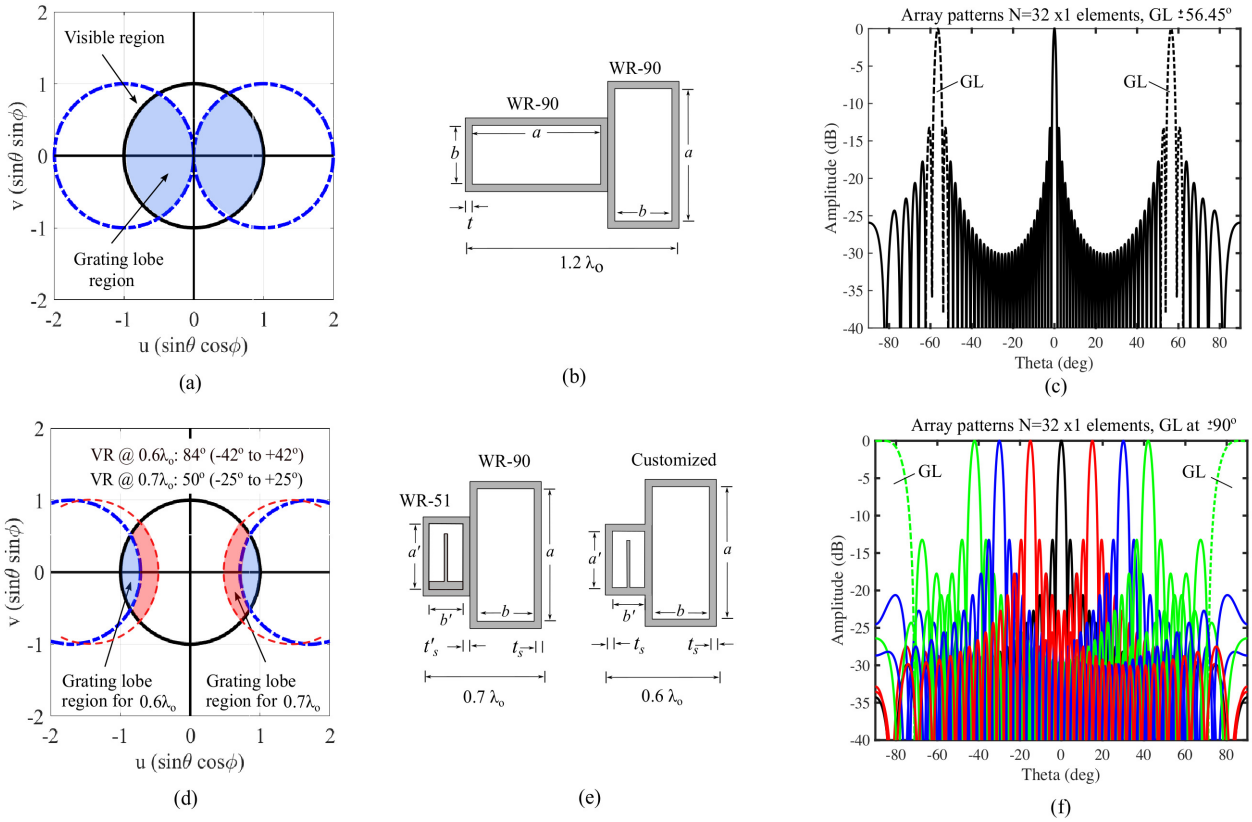

FIGURE 1: Grating lobe diagram using a conventional and proposed compact waveguide unit cell for dual-polarized array antenna. In (a-b) Grating lobe and dual-polarized unit cell based on convectional WR-90 waveguides, in this case unit cell spacing is $1.2\lambda_\circ$. (c) Array antenna pattern of 32x1 linear array with spacing of $1.2\lambda_\circ$. In (d-e) Grating lobe analysis for a dual-polarized unit cell based on proposed compact waveguides using standard waveguides; WR-51 for V-pol and WR-90 for H-pol for $0.7\lambda_\circ$ and $0.6\lambda_\circ$. (f) Array antenna pattern of 32x1 linear array with spacing of $0.6\lambda_\circ$. Grating lobe only appears after e-scanning is larger than $\pm 42^\circ$.

A. VERTICAL POLARIZATION LINEAR ARRAY

The partial H-plane waveguide is a rectangular waveguide with a quarter reduction in the cross-sectional area which is implemented by a concept of folded waveguide [20]. Recently, structures such as filters were designed based on partial H-plane waveguides. It has been widely utilized to design a compact waveguide filter named as a partial H-plane filter [21]. Nowadays, these structures are being used to design linear slotted waveguide array antennas with single polarization [22], [23].

The partial H-plane waveguide is a transversely folded rectangular waveguide that has a partially inserted metal vane in the H-plane [24]. The dominant and second modes of the rectangular waveguide are TE10 and TE20, respectively. Since these modes do not depend on the waveguide height, it is possible to reduce the height for these modes. Thus, the flat waveguide can be transversely folded once, which results in a quarter reduction in the cross-sectional area of the waveguide forming a compact structure. As shown in Fig. 2, the first two modes of a partial H-plane waveguide can have the same dispersion characteristics as those of a conventional rectangular waveguide, while its cross section is one quarter [25]. Therefore, both conventional and compact waveguides can achieve the same usable bandwidth. These two modes can be separately controlled if required for different applications. This new type of compact waveguide brings up numerous possibilities to use this waveguide for microwave applications that have space and weight limitations [22].

In [25], dispersion characteristics of the partial H-plane waveguides are theoretically investigated by applying Galerkin's method in Fourier domain to obtain the propagation constant and consequently, the fields in the structure.

The E-field distributions of dominant mode of conventional waveguide are the same as of the partial H-plane waveguide if it is unfolded with respect to the metal vane. Thus, a partial H-plane antenna can be constructed by using the same structure, broad wall longitudinal shunt slot, of conventional slot antenna.

For a longitudinal shunt slot on a conventional waveguide, a model of the antenna may be constructed by considering the slots as shunt admittances linked by sections of ideal transmission lines, shown in Fig. 3 [26], [27]. The active admittance of each slot in the slot array, Y_n^a, in the equivalent model usually includes both the self impedance, Y_n, and the effect of the mutual coupling with the remaining slots.

The procedure for the design of a linear array of longitu-

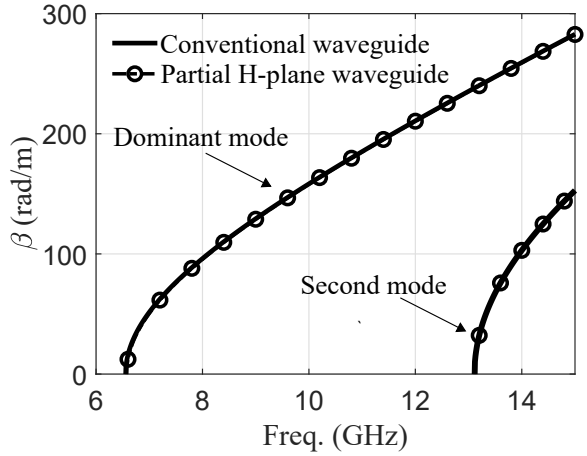

FIGURE 2: Dispersion characteristics of an X-band conventional rectangular waveguide with a = 22.86 mm and b = 10.16 mm and a partial H-plane rectangular waveguide (a = 11.43 mm, b = 6 mm, and metal vane height and thickness: 9.5 mm and 0.1 mm).

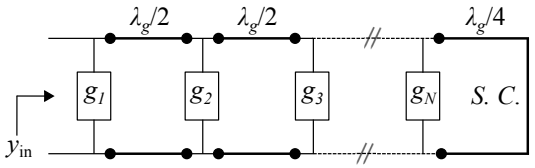

FIGURE 3: The equivalent circuit model of a resonant slotted waveguide array antenna with shunt conductances.

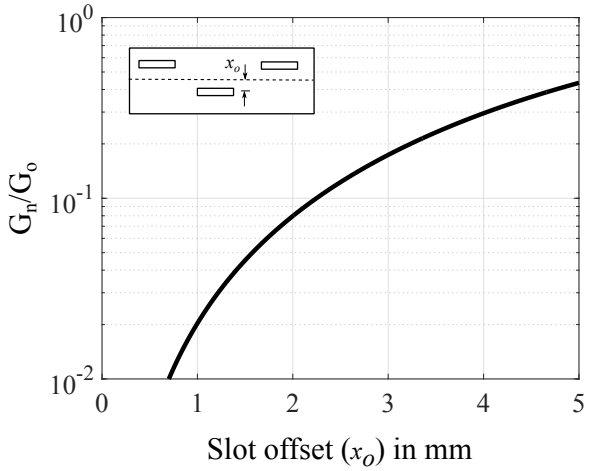

FIGURE 4: Normalized resonant conductance $g_n(x_0)$ vs. slot offset x_0 of isolated longitudinal shunt slot in a standard WR-90 (with a = 22.86 mm and b = 10.16 mm) at 9.4 GHz.

dinal slots fed by rectangular waveguide proposed by Elliott [8] depends on two design equations:

$$\frac{Y_s}{G_0} = -K_1 f(x_0, L)(\frac{V_s}{V_n}) \tag{3}$$

$$K_1 = -2\sqrt{\frac{Y_i}{G_0}}\frac{j\pi\sqrt{2}}{\beta_{10}k_0 a\sqrt{ab}} \tag{4}$$

$$f(x_0, L) = -\frac{\frac{\pi}{2kL}\cos(\beta_{10}L)}{(\frac{\pi}{2kL})^2 - (\frac{\beta_{10}}{k})^2}\cos(\frac{\pi x_0}{a}) \tag{5}$$

$$\frac{Y^a}{G_0} = \frac{2}{\frac{2}{\frac{Y_s}{G_0}} + \frac{1}{\Gamma}\frac{V_{scoupl}}{V_s}} \tag{6}$$

where Y_s is the admittance of the slot, G_0 is the characteristic conductance of the waveguide, x_0 is the slot offset, V_s is the slot voltage, V_n is the modal voltage at Y_s, $2L$ is the slot length.

The design equations will be solved iteratively; more details about the iterative design algorithm for standing wave arrays are presented in [8], [28]. The aim of the design procedure is to determine the length and offset of each slot in such a way as to achieve the desired voltage distribution on the different slots.

In [29], Stevenson derived a formula for the normalized resonant conductance of a single longitudinal slot as a function of its offset x_0 from the centerline as follows

$$\frac{G_s}{G_0} = 2.09\frac{a/b}{\beta/k}\cos^2(\frac{\beta\pi}{k})\sin^2(\frac{\pi x_0}{a}) \tag{7}$$

where G_s is the conductance of the slot.

The equation indicates that the normalized conductance of the longitudinal slot in the broad wall of a rectangular waveguide is offset dependent as shown in Fig. 4 using a standard WR-90 at 9.4 GHz. It is shown that by adjusting the slot offset from the center line of the waveguide, the slot conductance can be controlled and then the slot excitation.

The design of the partial H-plane slot array antenna is described in this section. The structure of 1-D resonant slot array antenna using the partial H-plane waveguide is shown in Fig. 6a,b. The slot length is nearly $0.5\lambda_\circ$, and its width is assumed to be very small. To be excited in phase for all slots, the array with slots spaced $0.5\lambda_g$ apart and with alternating slots on the opposite side of the center line is employed. The designed array follows the uniform array with a sidelobe level (SLL) of 13.26 dB, and the operation frequency is 9.4 GHz. The slot offsets of x_n's, which control the conductance and excitation level of each slot, are determined from the equation. The designed parameters are listed in Table 2. The thickness and width of each slot in the resonant slot array antenna are 1.27 mm and 1.533 mm, respectively. The thickness (d_4) and length (d_7) of the metal vane are set to be 0.5 mm and 9.5 mm, respectively. The longitudinal slot is cut in the narrow wall of the partial H-plane waveguide parallel

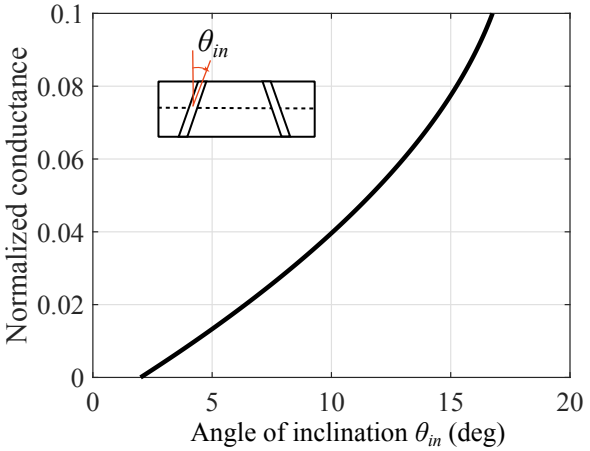

FIGURE 5: The variation of the normalized conductance with the angle of inclination of shunt slot in the narrow wall of a standard WR-90 with a = 22.86 mm and b = 10.16 mm at 9.4 GHz.

to the waveguide with an offset x_n = 2 mm from the center line. The polarization is perpendicular to the waveguide axis. The excitation is mainly controlled by the offset. It is the maximum at the edges and zero at the center. In order to radiate in the boresight, the longitudinal slot antennas are arrayed by a spacing of a half guided wavelength, and the offset direction is opposite among the adjacent slots.

A partial H-plane waveguide to coaxial adapter is used where a probe was inserted into a rectangular cut-out in the H-plane vane at the center of waveguide structure. The adapter was optimized using a commercial full wave simulator (HFSS) where the cut-out width and depth were optimized to maximize the return losses.

B. HORIZONTAL POLARIZATION LINEAR ARRAY

The second commonly used slot array antenna is the edge slot waveguide array antenna which has slots modified in sidewall of the waveguide to obtain a beam pattern in the H-plane. For an edge slot antenna, to obtain the desired shunt conductance value which is determined by a tilted angle of sidewall slot, the slot is cut into the sidewall and wrapped around the broad wall of the waveguide because the height of the sidewall of the conventional waveguide is usually smaller than the resonant length of the slot. Each slot is approximately half a free space wavelength long and is spaced by a half guided wavelength from its adjacent slots at the design frequency if a standing wave feed is used to obtain a radiating element of in-phase. In order to excite each slot with in-phase spaced by a half guided wavelength, the adjacent slots in sidewall are oppositely inclined with respect to the vertical centerline.

In [29], Stevenson derived the values of the resonant conductance, normalized to the waveguide conductance, for a slot in the narrow wall of the rectangular waveguide using transmission-line theory and the waveguide modal Green's functions. The conductance of narrow wall (edge) shunt slot is given by

$$\frac{G_s}{G_0} = \frac{30}{73\pi}\frac{\lambda_g}{\lambda_\circ}\frac{\lambda_\circ^4}{a^3 b}\left(\frac{\sin\theta_{in}\cos(\frac{\pi\lambda_\circ}{2\lambda_g}\sin\theta_{in})}{1-(\frac{\lambda_\circ}{\lambda_g})^2\sin^2\theta_{in}}\right)^2 \quad (8)$$

where θ_{in} is the inclined angle of the slot relative to the vertical direction 'b'.

As shown in Fig. 5, with increasing the inclination angle, the slot conductance in the narrow wall of the WR-90 waveguide increases.

The reason for the inclination is that the non-inclined slot disrupts a negligible current in the narrow wall of the waveguide when TE10 dominant mode propagates inside the waveguide. Consequently, the slot will not radiate because a very week electric field is excited in the slot. However, the inclined slot does interrupt the wall current by an amount controlled by the slot tilt. Unfortunately, the excitation technique applied to the edge wall slots using the inclination has some drawbacks. In addition to the desired longitudinally polarized electric field, the inclination produces a vertically polarized electric field, which is often undesirable. The presence of the unwanted polarization increases the cross-polarization levels.

Non-inclined narrow-wall slots in the waveguide generate the horizontal polarization with suppressed cross-polarization. The slots have to extend into the neighboring broad walls of the waveguide to be resonant. The edge slots in the narrow wall need to be excited with a pair of irises inside the waveguide and not by slot tilt in order for minimum cross-polarization generation. The excitation of the edge slots is controlled by the iris dimensions and locations.

The structure of 1-D resonant slot array antenna using non-inclined narrow-wall slots in the conventional waveguide is shown in Fig. 6a,b. To be excited in phase for all slots, the array with slots spaced $0.5\lambda_g$ apart and with two excitation irises at each side of the slot sitting on opposite broad walls is employed. The designed array follows the uniform array with a sidelobe level (SLL) of 13.26 dB, and the operation frequency is 9.4 GHz. The designed parameters are listed in Table 2. The thickness and width of each slot in the resonant array antenna is 1.27 mm and 1.533 mm, respectively. The polarization is parallel to the waveguide axis. The iris's dimensions and locations, used to excite the slots, are optimized and the obtained values are listed in Table 2.

The design of a linear slotted waveguide array antenna begins by determining the aperture distribution, and hence the slot excitation, required to achieve the beamwidth, gain, and sidelobe level needed at the center frequency. The radiated power and resonant conductance of a slot is proportional to the square of the voltage excitation of the slot. The normalized resonant conductance g_n of the nth slot, for a given aperture voltage distribution, is given by

$$g_n = \frac{a_n^2}{\sum_{i=1}^{N} a_i^2} \quad (9)$$

where, N is the number of slots in a linear array, and a_n

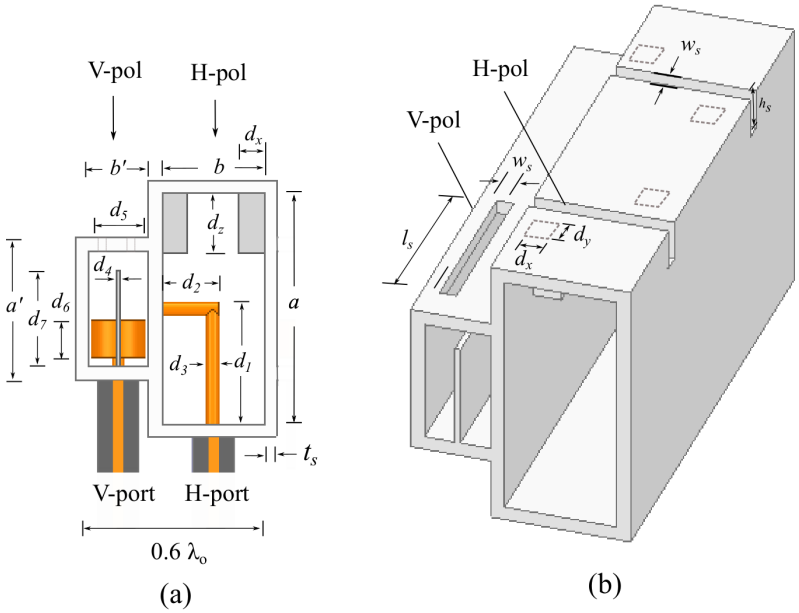

FIGURE 6: Geometry of proposed dual-polarized slotted waveguide antenna unit cell. (a) Side view of dual-polarized element and feed structure, and (b) 3D view of dual-polarized antenna element.

TABLE 2: Summary of the dimensions of V-pol and H-pol linear slotted waveguide array antennas.

	Cross section (mm × mm)	Frequency (GHz)	Slot (mm)						Iris dimensions (mm)		
	$a \times b$	$f_\circ$	l_s	w_s	t_s	h_s	x_n	l_g	dx	dy	dz
H-pol	22.68×10.16	9.4	–	1.533	1.27	3.75	–	22.2704	2.5	2.5	6.5
V-pol	11.43×6	9.4	15.4	1.533	1.27	–	2	22.2704	–	–	–

TABLE 3: Radiation parameters of the dual-polarization slotted waveguide array antenna with eight slots.

Type	Bandwidth (%)	Gain (dBi)	SLL (dB)	Cross-polarization level (dB)
Conventional antenna (H-pol)	2.23	16.72	12.96	-60
Compact antenna (V-pol)	2.29	17.23	14.65	-60

is the voltage excitation for the nth slot. For the uniform illumination, g_n=1/N.

Once the the slot conductance is obtained based on its voltage excitation, the slot placement and orientation can be calculated using (3-8).

Performance of the antenna unit cell (8-slot linear array) is analyzed using HFSS. The S-parameters and gain of the basic unit of both V- and H-polarizations are depicted in Fig. 7a,b. The reflection coefficients of the VP and HP units are lower than -10 dB over the frequency range from 9.3 GHz to 9.5 GHz. The bandwidth for $|Svv|$ (or $|Shh|$) $<$ -10 dB is about 2.3% (9.3 GHz – 9.5 GHz). The isolation ($|Shv|$) between the V- and H-ports of the antenna is higher than 60 dB. In addition, the realized gain of the proposed antenna versus the frequency is exhibited in Fig. 7b. It is shown that the variation of the gain for both polarizations over the frequency bandwidth is about 0.5 dB.

Fig. 7c,d shows the co- and cross-polarization gain radiation patterns at several frequencies in the band (9.3 GHz, 9.4 GHz and 9.5 GHz) in elevation plane (along the waveguide axis) of H-pol array antenna and V-pol array antenna, respectively. The unit cell has two arrays for V-pol and one array for H-pol to have close effective aperture. It is observed that the radiation patterns of both antennas are stable over the frequency band. The maximum SLL is –13 dB with cross-polarization level of -60 dB below the main lobe for both HP and VP arrays. Performance comparison of the linear array antenna for both polarizations (H and V) is summarized in Table 3.

C. DUAL-POLARIZED PLANAR ARRAY ANTENNA

The structure of the dual-polarization planar SWGAs array is shown in Fig. 8a,b. With the VP and HP linear arrays designed using HFSS, the dual-polarization planar array antenna is composed of a 8x8 VP sub-array and a 8x8 HP sub-array. When the vertical polarization linear array is designed, the effect of the horizontal polarization array is considered, and vice versa. Both waveguides used for the VP and HP linear arrays have the same guided wavelength, thus both antennas have the same length. In the back, at the centers of the linear arrays, 50Ω probe adapters for both polarizations are arranged. It is arranged with HP and VP waveguide arrays side by side, eight linear arrays for each, in which the HP waveguide linear arrays are higher than the VP waveguide

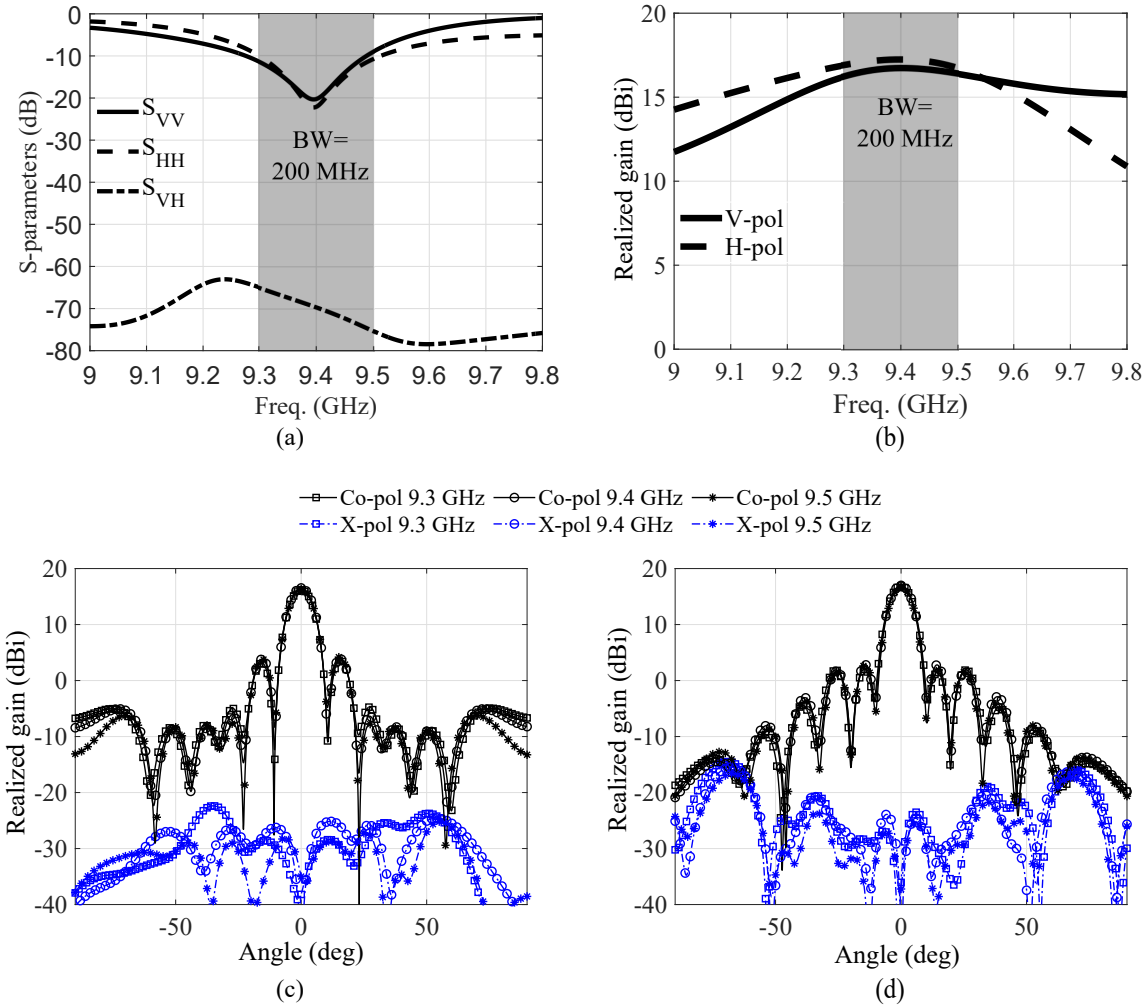

FIGURE 7: (a) S-parameters of the proposed dual-polarization antenna (b) Realized gain values verses the frequency for V-pol antenna and H-pol antenna (c) Co- and cross-polar gain radiation patterns at 9.3 GHz, 9.4 GHz and 9.5 GHz of H-pol antenna in the E-plane (d) Co- and cross-polar gain radiation patterns at 9.3 GHz, 9.4 GHz and 9.5 GHz of V-pol antenna in the H-plane.

linear arrays, as shown in Fig. 8b. The width of two linear arrays together is up to $0.58\lambda_\circ$ in order to obtain a $\pm 42^\circ$ beam scanning.

The simulated radiation pattern scanning performances of the proposed planar array antenna for both polarizations in the azimuth plane perpendicular to the waveguide axis at 9.4 GHz with uniform illumination are shown in Fig. 8c,d. The main beam direction can scan from -45° to $+45^\circ$ with a step of 15°. At the maximum scanning angle of $\pm 45^\circ$ in the E-plane of the V-polarization array antenna, the gain decreases by 3.2 dB, meanwhile the sidelobe degradation is 1 dB. However, in the H-plane of the H-polarization array antenna, the gain decreases 2.6 dB and the sidelobe degradation is 1.0 dB when the scanning angle reaches $\pm 45^\circ$. Another advantage of this design configuration is a high polarization purity in all scanning angles with the cross-polarization level better than -60 dB in the main beam directions. We can also observe that the sidelobe levels in all scanning angles are lower than 13 dB. The array also enables individual excitation for each 1x8 element sub-array. Amplitude tapering can be applied using a 6-bit attenuator for sidelobe reduction. The radiation pattern scanning performances of the proposed planar array antenna, using a Taylor 25 dB ($\bar{n}$=3) amplitude distribution, for V- and H-polarizations in the azimuth plane perpendicular to the waveguide axis at 9.4 GHz are depicted in Fig. 8e,f. For both VP and HP, the main beam is scanned from -45° to $+45^\circ$ with a step of 15°. At the maximum scanning angle of $\pm 45^\circ$ in the E-plane of the V-polarization array antenna, the gain decreases by 3.2 dB, meanwhile the sidelobe degradation is 1 dB. However, in the H-plane of the H-polarization array antenna, the gain decreases by 2.6 dB and the sidelobe degradation is 1.0 dB when the scanning angle reaches $\pm 45^\circ$. It can be seen that the maximum SLL is –24.5 dB with cross-polarization level of -60 dB below the main lobe for HP array. The maximum SLL is –25 dB with cross-polarization level of -60 dB below the main lobe for VP array. In order to design a dual-polarization slotted waveguide array antenna with low SLL, a tapering amplitude distribution is required.

The desired amplitude distribution is a two parameter Taylor distribution with 8 elements, ñ=3 and sidelobe level of -25 dB. The definition of the parameter ñ and the details of the Taylor distribution can be found in [30].

Fig. 9 illustrates the overlapped normalized e-scanned gain of the 8x8 array antenna at 9.4 GHz. Co-polar pattern mismatch and cross-polarization isolation are key metric parameters for dual-polarimetric radars used in weather application. In this application, cross-polarization isolation is below -40 dB, and less than $\pm$ 0.2 dB is the maximum tolerable mismatch between H- and V-polarization co-polar patterns [1], [2]. Using this proposed design, a cross-polarization level below -60 dB and a co-polar pattern mismatch around $\pm$0.12 dB were obtained over a scanning range of 84° ($\pm$42°).

The proposed array unit cell of 8x8 elements can be easily integrated with active modules for 1D e-scanning capability. This active array can be used to create a large aperture array for 2°x2° antenna beamwidth. Conventional or customized electronics using GaAs or GaN can be used for the front-end modules (FEC), where power levels from 1 to 20 Watts per 8-element sub-array can be easily obtained. RF-CMOS technology is commercially available for control module (CM). CMOS technology enables high integration of 7-bit digital phase shifters, 7-bit digital attenuators, high isolation T/R and polarization switches and gain blocks [31], [32]. The proposed solution with active components is very attractive for airborne and weather radar applications that require 1D e-scanning beam patterns, high power and high polarization purity.

D. FEEDING TECHNIQUE AND STRUCTURE

The standard rectangular waveguides are preferably used as transmission lines for high power applications. Like other transmission lines, these waveguides have a characteristic impedance which requires matching for maximum power transfer. Therefore, there is a need for an adapter between 50Ω coaxial cables and the rectangular waveguides, a so-called coax-to-waveguide adapter. This adapter will introduce the coaxial cable mode to the rectangular waveguide mode. Coupling loops and probes are common ways to inject or remove microwave signal to the waveguide. The probes couple to an electric field of a certain mode inside the waveguide and the loops couple to a magnetic field of the same mode, but both an electric and a magnetic field will be set up in each case because the two are inseparable. The majority of commercially available coax-to-waveguide adapters are monopole probes. Resonantly-fed slotted waveguide array antennas have been in use for a long time. The end feed and center feed are the most common ways to feed the one-dimensional slotted waveguide array antennas with standing-wave excitation. In the end feed configuration, the waveguide array antenna is fed from one end of the waveguide and terminated by a short circuit at the other end. The feed needs to be positioned at odd multiples of $\lambda_g/4$ or $\lambda_g/8$ at the center frequency from the waveguide feeding end and the short circuit is $\lambda_g/4$ away from the end slot. The normalized conductance of the end-fed slotted waveguide array antennas for the matching conditions at the feed is given by

$$\sum_{n=1}^{N} g_n = 1 \tag{10}$$

where N is the number of slots in the waveguide, and g_n is the normalized conductance of the slot nth.

The center feed is another popular way to feed the one-dimensional slotted waveguide array antennas where the antenna waveguide is fed from the center and is terminated by short circuits $\lambda_g/4$ away from both end slots. A center feed configuration is introduced to enhance the bandwidth as well as to suppress the frequency dependent beam squinting [33]. In addition, more compact antenna system with symmetrical radiation patterns is obtained. Similarly, the matching condition at the feed is given by

$$\sum_{n=1}^{N} g_n = 2 \tag{11}$$

In this work, the center feed configuration is selected to feed both conventional and partial H-plane waveguides. For the V-polarization array antenna, the slotted partial H-plane waveguide is used. A coaxial to partial H-plane waveguide adapter with a conducting disc attached to the end of the probe is used where a probe was inserted into a rectangular cut-out in the H-plane vane at the center of the waveguide. And a hole is drilled in the bottom wall of the waveguide to insert the probe into the waveguide. The diameter d_p and length l_p of the probe, the diameter d_5 and thickness d_6 of the disc, and the rectangular cut dimensions w_c, h_c will influence the impedance matching between the coaxial transmission line and the partial H-plane waveguide. The transition structure has been optimized using a commercial HFSS simulator to realize the input impedance requirements and the obtained values of all parameters are presented in Table 4.

For the H-polarization array antenna, L-loop side launcher coaxial-to-waveguide transition is used to inject energy into a waveguide by setting up an H-field in the waveguide. By L-shape loop coupling in a rectangular waveguide first a H-field is produced which causes an E-field. A hole is drilled in the narrow wall of the waveguide to insert the probe into the waveguide and the L-loop is formed by soldering the coaxial probe onto the broad wall of the waveguide and is used to generate a current loop, then the current loop becomes a proper excitation for the magnetic field of the dominant TE10 mode. A simple L-shape transition structure has been optimized using a commercial HFSS simulator to realize the input impedance requirements and the obtained values of all parameters are presented in Table 4.

As depicted in Table 5, the proposed ultra compact high performance slotted waveguide array antenna is compared with the previous customized slotted waveguide antenna structures. The proposed antenna has better cross-polarization isolation and large scanning range because of

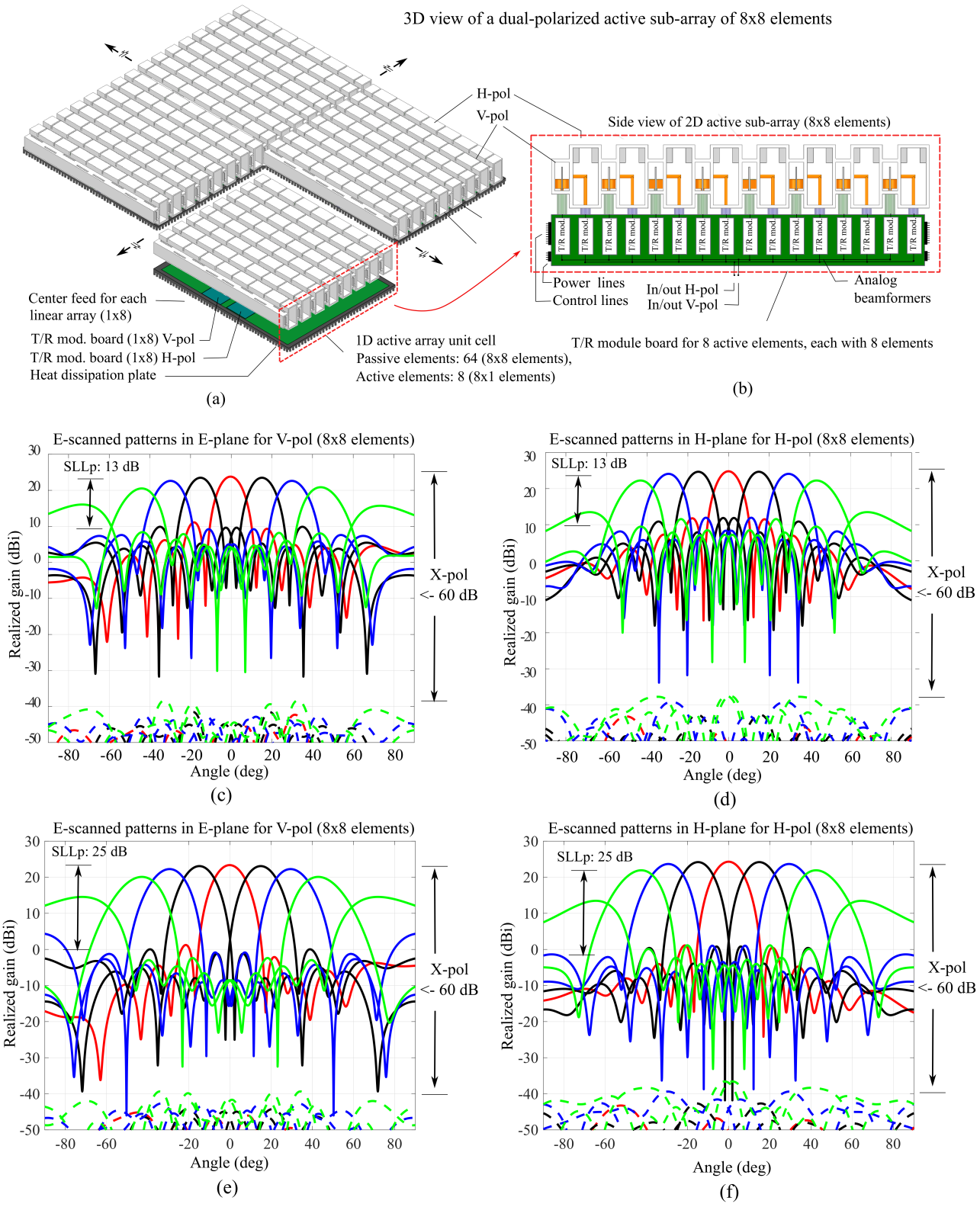

FIGURE 8: Geometry of proposed active dual-polarized planar SWGA array antenna (a) 3D view; (b) Side view of the feeding structure. Simulated co- and cross-polarization patterns scanning characteristics at 9.4 GHz with various scan angles θ_s = $\pm 0^\circ$, $\pm 15^\circ$, $\pm 30^\circ$, $\pm 45^\circ$ (c) E-plane of V-polarization antenna with uniform illumination; (d) H-plane of H-polarization antenna with uniform illumination (e) E-plane of V-polarization antenna with tapered illumination; (f) H-plane of H-polarization antenna with tapered illumination.

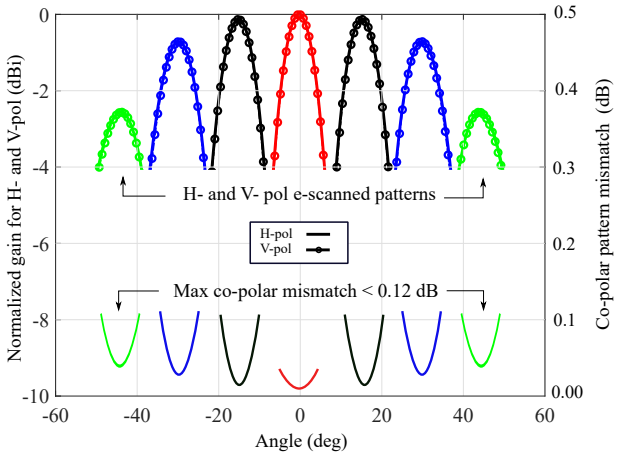

FIGURE 9: Simulated co-polar pattern mismatch at 9.4 GHz with uniform illumination at various scan angles θ_s = $\pm 0^\circ$, $\pm 15^\circ$, $\pm 30^\circ$, $\pm 45^\circ$.

TABLE 4: Summary of the dimensions of H- and V-polarization feeding structures.

H-polarization array	**L-shape probe (mm)**					
	d_3	d_1	d_3	d_2		
	1.27	11.43	1.27	5.08		
V-polarization array	**Disc-shape probe (mm)**					
	d_p	l_p	d_5	d_6	w_c	h_c
	1.27	1	5.5	3.25	8	4.25

TABLE 5: Comparison of previous and proposed work.

Parameters	**Ref [14]**	**Ref [15]**	**This work**
Frequency band	X-band	L-, C-band	X-band
Bandwidth (MHz)	300	200	200
Waveguide types	Partially customized	Fully customized	Standard ($0.7\lambda_\circ$) Customized ($0.6\lambda_\circ$)
Element spacing	$0.7\lambda_\circ$	$0.7\lambda_\circ$	$0.7\lambda_\circ$ $0.6\lambda_\circ$
Max. scanning range	40° ($\pm 20^\circ$)	40° ($\pm 20^\circ$)	84° ($\pm 42^\circ$)
Cross-pol isolation	<-40 dB	<-30 dB	<-60 dB
Co-pol mismatch	NA	NA	< 0.12 dB

the element spacing reduction of the proposed structure. In addition, the proposed design discussed about the co-polar pattern mismatch (<-0.12 dB), which is the critical parameter for dual-polarization applications. The only trade-off of the proposed structure is the narrow bandwidth compare to [14].

IV. CONCLUSION

The design of an X-band dual-polarized planar slotted waveguide antenna (SWGA) array is presented. This design provides very high isolation between V- and H-ports over 200 MHz bandwidth and wide-angle scanning performance in the azimuth plane. The proposed design uses a compact array unit cell where the overall dimensions are reduced to 50% in comparison with that of the dual-polarization slotted waveguide array antenna using the conventional rectangular waveguides. This design overcomes the fundamental limitation of zero electronically scanning, due to large element spacing ($1.2\lambda_\circ$), when conventional waveguides are used. Reducing the element spacing to $0.6\lambda_\circ$ (in the azimuth plane), based on a partial H-plane waveguide, enables a 1D e-scanning range up to $84^\circ(\pm 42^\circ)$ in the azimuth plane perpendicular to the waveguide axis. The design uses longitudinal shunt slots on the partial H-plane waveguide for V-polarization antenna and non-inclined edge wall slots on the conventional waveguide for H-polarization antenna. Results demonstrate 200 MHz bandwidth centered at 9.4 GHz (2.2 % fractional bandwidth), in terms of radiation patterns and input impedance match. Sidelobe level can be synthesized using the attenuators for each sub-array (1x8 elements) in azimuth plane. The polarization purity of the antenna is excellent with a cross-polarization level better than -60 dB at the boresight and scanned patterns up to $\pm 45^\circ$. An active sub-array panel of 8×8 elements, excited with 8 high-power transmit and receive modules are proposed. This active sub-array can be scaled to obtain a large array without any constrains in size and power.

ACKNOWLEDGMENT

The authors would like to thank the Agile RF Systems LCC for partially support of this work. Also thanks to the Advanced Radar Research Center (ARRC) of The University of Oklahoma for providing the facilities needed to perform this research. They are also thankful to all members of the Phased Array Antenna Research and Development (PAARD) group for the discussions and positive feedback.

REFERENCES

[1] D. Zrnic and R. Doviak, "System Requirements for Phased Array Weather Radar," NOAA/NSSL, Tech. Rep., 2005.
[2] Y. Wang and V. Chandrasekar, "Polarization Isolation Requirements for Linear Dual-polarization Weather Radar in Simultaneous Transmission Mode of Operation," IEEE Transactions on Geoscience and Remote Sensing, vol. 44, no. 8, pp. 2019–2028, 2006.
[3] J. Knorr, "Analysis of Performance Characteristics of the MWR-05XP Mobile Weather Radar," pp. 1–51, 2005.
[4] Y. Chen and R. Vaughan, "Dual-polarized L-band and Single-polarized X-band Shared-aperture SAR Array," IEEE Trans. on Antennas and Propag., vol. 66, no. 7, pp. 3391–3400, 2018.
[5] J. Díaz, J. Salazar, J. Ortiz, C. Fulton, N. Aboserwal, R. Kelley, and R. Palmer, "A Dual-polarized Cross-stacked Patch Antenna with Wide-angle and Low Cross-polarization for Fully Digital Multifunction Phased Array Radars," IEEE International Symposium on Phased Array Systems and Technology (PAST), pp. 1–4, 2016.
[6] R. Hansen, "Phased Array Antennas, 2nd ed." John Wiley Sons, Inc., Hoboken, New Jersey, 2009.
[7] K.-L. Hung and H.-T. Chou, "A Design of Slotted Waveguide Antenna Array Operated at X-band," IEEE International Conference on Wireless Information Technology and Systems, pp. 1–4, 2010.
[8] L. Josefsson and S. Rengarajan, "Slotted Waveguide Array Antennas: Theory, Analysis and Design," SciTech Publishing, 2018.
[9] C. Ahsan and D. Vakula, "Non-inclined Slotted Waveguide Array with Various Shapes of Irises," International Journal of Advanced Engineering, Management and Science, vol. 2, no. 6, pp. 655–658, 2016.
[10] S. Hashemi and R. Elliott, "Analysis of Untilted Edge Slots Excited by Tilted Wires," IEEE Trans. Antennas Propag., vol. 38, no. 11, pp. 1737–1745, 1990.
[11] Y. Yuan, Z. Xu, and X. Yan, "Analysis of Shaped-differ Impelled-pins in Edge Wall Waveguide Slot," 5th IEEE International Symposium on Microwave, Antenna, Propagation and EMC Technologies for Wireless Communications, pp. 323–326, 2013.
[12] A. G. Derneryd and A. Lagerstedt, "Novel Slotted Waveguide Antenna with Polarimetric Capabilities," International Geoscience and Remote Sensing Symposium, IGARSS, vol. 3, pp. 2054–2056, 1995.
[13] T. Li, H. Meng, and W. Dou, "Design and Implementation of Dual-frequency Dual-polarization Slotted Waveguide Antenna Array for Ka-

band Application," IEEE Antennas and Wireless Propagation Letters, vol. 13, pp. 1317–1320, 2014.
[14] W. Wang, J. Jin, J. Lu, and S. Zhong, "Waveguide Slotted Antenna Array with Broadband, Dual-polarization and Low Cross-polarization for X-band SAR Applications," IEEE International Radar Conference, pp. 1–4, 2005.
[15] M. Chen, X. Fang, W. Wang, H. Zhang, and G. Huang, "Dual-band Dual-polarized Waveguide Slot Antenna Array for SAR Applications," IEEE Antennas and Wireless Propagation Letters, vol. 19, no. 10, pp. 1719–1723, 2020.
[16] Z. Yu-mei, Z. Zu-ji, and L. Xiao-peng, "Design of Ultralow Sidelobe Antenna Arrays with Inclined Slots in the Narrow Wall of Rectangular Waveguide," Proceedings of the International Conference on Radar, pp. 437–441, 2003.
[17] E. Cullens, L. Ranzani, K. Vanhille, E. Grossman, N. Ehsan, and Z. Popovic, "Micro-fabricated 130-180 GHz Frequency Scanning Waveguide Arrays," IEEE Trans. Antennas Propag., vol. 60, no. 8, pp. 3647–3653, 2012.
[18] R. Camblor, S. Ver Hoeye, C. V´azquez, G. Hotopan, M. Ferna´ndez, and F. Las Heras, "Sub-millimeter Wave Frequency Scanning 8×1 Antenna Array," Progress in Electromagnetic Research PIER, vol. 132, pp. 215–232, 2012.
[19] R. Mailloux, "Phased Array Antenna Handbook, 2nd ed." Artech House, 2005.
[20] D. Kim and J. Lee, "A Partial H-plane Waveguide as a New Type of Compact Waveguide," Microwave and Optical Technology Letters, vol. 43, no. 5, pp. 426–429, 2004.
[21] D. W. Kim, D. J. Kim, and J. Lee, "Compact Partial H-plane Filters," IEEE Trans. on Microwave Theory and Tech., vol. 54, no. 11, pp. 3923–3930, 2006.
[22] D. Kim and J. Lee, "Compact Resonant Slot Array Antenna Using Partial H-Plane Waveguide," IEEE ANTENNAS AND WIRELESS PROPAGATION LETTERS, vol. 9, pp. 530–533, 2010.
[23] ——, "Resonant Array Antenna Using Inclined Sidewall Slot in Partial H-plane Waveguide," IRMMW-THz Symposium, pp. 1–2, 2009.
[24] ——, "Partial H-plane Filters with Partially Inserted H-plane Metal Vane," IEEE Trans. Micro. Wireless Compon. Letters, vol. 15, no. 5, pp. 351–353, 2005.
[25] R. Rezaiesarlak, E. Mehrshahi, and M. Gharib, "Dispersion Characteristics of Partial H-plane Waveguides," Progress in Electromagnetics Research Letters, vol. 24, pp. 51–58, 2011.
[26] L. K. R. Elliott, "The Design of Small Slot Arrays," IEEE Trans. Antennas Propag., vol. AP-26, no. 2, pp. 214–219, 1978.
[27] G. Stern and R. Elliot, "Resonant Length of Longitudinal Slots and Validity of Circuit Representation: Theory and Experiment," IEEE Trans. Antennas Propag., vol. 33, no. 11, pp. 1264–1271, 1985.
[28] R. S. Elliott, "An Improved Design Procedure for Small Arrays of Shunt Slots," IEEE Trans. Antennas Propag., vol. AP-31, no. 1, pp. 48–53, 1983.
[29] A. Stevenson, "Theory of Slots in Rectangular Waveguides," J. Appl. Phys., pp. 24–38, 1948.
[30] C. Balanis, "Antenna Theory: Analysis and Design, 4td ed." John Wiley Sons, Inc., Hoboken, New Jersey, 2016.
[31] J. Ortiz, J. Salazar-Cerreno, D. Díaz, M. Lebrón, N. Aboserwal, and L. Jeon, "Low-cost CMOS Active Array Solution for Highly-dense X-band Weather Radar Network," IEEE Trans. on Antennas and Propag., vol. 68, no. 7, pp. 5421–5430, 2020.
[32] J. Salazar, R. Medina, and E. Loew, "Transmit/receive (T/R) Modules Architectures for Dual-polarized Weather Phased Array Radars," in IEEE MTT-S International Microwave Symposium, 2015, pp. 1–4.
[33] M. Muller, I. Theron, and D. Davidson, "Improving the Bandwidth of a Slotted Waveguide Array by Using a Center-feed Configuration," 1999 IEEE Africon. 5th Africon Conference in Africa, pp. 1075–1080, 1999.

NAFATI ABOSERWAL (S'13-M'16) received the B.S. degree in Electrical Engineering from Al-Mergheb University, Alkhoms, Libya, in 2002. He received his M.S. and Ph.D. degrees in Electrical Engineering from Arizona State University, Tempe, AZ, in 2012 and 2014, respectively. In January 2015, he joined the Advanced Radar Research Center (ARRC) and the Department of Electrical and Computer Engineering at The University of Oklahoma (OU), Norman, as a Postdoctoral Research Scientist. Currently he is a Research Associate and a Manager of Far-Field, Near-Field and Environmental Anechoic Chambers at the Radar Innovations Laboratory (RIL). His research interests include EM theory, computational electromagnetics, antennas, and diffraction theory, edge diffraction and discontinuities impact on the array performance. His research also focuses on active high performance phased array antennas for weather radars, higher modes and surface waves characteristics of printed antennas, and high performance dual-polarized microstrip antenna elements with low cross-polarization. Dr. Aboserwal is a member of the IEEE Antennas and Propagation Society (AP-S)

JORGE L. SALAZAR-CERRENO (S'00-M'12-S'14) received a B.S. In ECE from the University Antenor Orrego, Trujillo, Peru, M.S. degree in ECE from the University of Puerto Rico, Mayagüez (UPRM). In 2011, he received his Ph.D. degree in ECE from the University of Massachusetts, Amherst. His Ph.D. research focused on development of low-cost dual-polarized active phased array antennas (APAA). After graduation, Dr. Salazar-Cerreno was awarded a prestigious National Center for Atmospheric Research (NCAR) Advanced Study Program (ASP) postdoctoral fellowship. At NCAR, he worked at the Earth Observing Laboratory (EOL) division developing airborne technology for two-dimensional, electronically scanned, dual-pol phased array radars for atmospheric research. In July 2014, he joined the Advanced Radar Research Center (ARRC) at The University of Oklahoma as a research scientist, and became an assistant professor at the School of Electrical and Computer Engineering in August 2015. His research interests include high-performance, broadband antennas for dual-polarized phased array radar applications; array antenna architecture for re-configurable radar systems; APAA; Tx/Rx modules; radome EM modeling; and millimeter-wave antennas. In 2019, Dr. Salazar was awarded the prestigious William H. Barkow Presidential Professorship from The University of Oklahoma for meeting the highest standards of excellence in scholarship and teaching. Dr. Salazar is He is a senior member of the IEEE Antennas and Propagation Society (AP-S), and a reviewer of various IEEE and AMS conferences and journals.

ZEESHAN QAMAR (S'11-M'17) received the B.Sc. and M.Sc. degrees in electrical engineering from the COMSATS University, Islamabad, Pakistan, in 2010 and 2013, respectively, and the Ph.D. degree in electronic engineering from the City University of Hong Kong, Hong Kong, in 2017. From Jul. 2010 to Aug. 2013, he was a Research Associate with the Department of Electrical and Computer Engineering, COMSATS University. From Nov. 2017 to Apr. 2018, he was a Postdoctoral Research Associate with the Department of Materials Science and Engineering, City University of Hong Kong. He is currently a Post- Doctoral Research Fellow with the Phased Array Antenna Research and Development group (PAARD) and the Advanced Radar Research Center (ARRC) at The University of Oklahoma, Norman, OK, USA. His current research interests include microwave/millimeter-wave circuits, material characterization, meta-materials, artificial dielectric layer, antennas and phased arrays, phased array antennas. He is a member of the IEEE Antennas and Propagation Society (AP-S), and a reviewer of various IEEE and IET conferences and journals.